

## Reversed quantum-confined Stark effect and an asymmetric band alignment observed for type-II Si/Ge quantum dots

M. Larsson, P. O. Holtz, A. Elfving, G. V. Hansson, and W.-X. Ni

*IFM, Department of Physics, Linköping University, S-581 83 Linköping, Sweden*

(Received 4 November 2004; published 2 March 2005; publisher error corrected 8 March 2005)

We report on the quantum-confined Stark effect for spatially indirect transitions in Stranski-Krastanov grown type-II Si/Ge quantum dots. A linear blueshift of the spatially indirect transition is observed at increasing electric field in contrast to the commonly observed redshift for type-I transitions. A shift of the emission-peak position and different quenching rates of the photoluminescence for *p-i-n* and *n-i-p* diodes at increased electric field and temperature indicate a deeper notch potential for electrons above the dot than below due to a strain-induced asymmetry in the band alignment.

DOI: 10.1103/PhysRevB.71.113301

PACS number(s): 78.67.Hc, 73.21.La, 78.55.Ap, 81.07.Ta

It has been shown that the poor optical properties of Si and Ge, due to indirect band gaps, can be improved by utilizing low-dimensional Si/Ge structures, e.g., quantum dots (QDs).<sup>1</sup> In such structures, the alloy disorder and quantum-confinement effects relax the *k*-conservation conditions sufficiently to increase the probability for optical recombination. Epitaxial growth of the lattice mismatched Si/Ge material system has been demonstrated to proceed via the Stranski-Krastanov mode under certain growth conditions.<sup>1,2</sup> As a result, self-assembled Ge QDs embedded in Si matrices can be produced in a way that is compatible with the Si technology. Accordingly, it is important to further investigate the optical transitions and carrier dynamics related to the Ge dots in the development of Si-based optoelectronic devices. In spite of the fact that Si/Ge interdiffusion will lead to some alloying of the dots we will refer to them as Ge dots.

When an electric field is applied along a quantization direction of a quantum structure, the potentials in the structure are tilted, causing a shift of the transition energy, the quantum-confined Stark effect (QCSE).<sup>3</sup> For type-I systems, the QCSE causes a quadratic redshift of the transition energy.<sup>3,4</sup> Prior to our study, no experimental evidence for QCSE in Stranski-Krastanov grown Si/Ge QDs has been shown. In contrast to the normally observed redshift, we report on a linear blueshift of the spatially indirect transition with increasing electric field, which is characteristic for type-II systems. In order to probe the QCSE in both field directions, measurements were performed on reversed biased *p-i-n* and *n-i-p* diodes, i.e., diodes with the top layer being *n*-doped and *p*-doped, respectively. Furthermore, since the *p-i-n* and *n-i-p* structures have their built-in electric fields in opposite directions, we were able to observe the difference between the conduction-band (CB) offsets at the top and bottom interfaces of the Ge dot by comparing the luminescence properties of the two diodes. The photoluminescence (PL) from transitions that involves electrons located above the Ge dot survives to higher temperatures and higher electric fields than the luminescence originating from the electrons below the dot, consistent with an asymmetric energy-band lineup.

In Si/Ge QDs, the confinement of the electrons is a result of tensile strain in the Si surrounding the Ge dot.<sup>1,2,5</sup> Our results show that the notch potential for electrons at the in-

terface above the Ge dot is deeper than the one underneath, and this is attributed to an asymmetric strain profile. Such asymmetric strain profiles through self-assembled QD structures have several times been predicted by theoretical calculations.<sup>5-7</sup> The type-II band alignment in the Si/Ge material system provides the possibility to study this effect in QDs and this is an experimental confirmation of the asymmetric strain and hence the asymmetric band alignment in Si/Ge QD structures.

As mentioned above, both *p-i-n* and *n-i-p* diodes were produced in order to study the QCSE in both field directions. To be able to compare the two different structures, the intrinsic layer of the two diodes were grown using identical growth sequences. The samples were grown by solid-source molecular-beam epitaxy (MBE) at a growth temperature of 530 °C. The *p-i-n* structure was grown on a *p*-doped Si(100) substrate ( $5 \times 10^{18} \text{ cm}^{-3}$ ) and the *n-i-p* on an *n*-doped Si(100) substrate ( $1 \times 10^{19} \text{ cm}^{-3}$ ). Ten Ge dot layers, each separated by a 60-nm-thick Si spacer, were incorporated in the intrinsic region. Each dot layer was formed via the Stranski-Krastanov growth mode as a result of an 8-ML deposition of Ge on the Si surface. The lateral size of the dots was 20–30 nm and the height was about 2–3 nm, as determined from AFM measurements. The *p-i-n* (*n-i-p*) structure was capped with a 200 nm *n*-doped (*p*-doped) layer ( $5 \times 10^{16} \text{ cm}^{-3}$ ). Finally, a 160-nm contact layer ( $2 \times 10^{18} \text{ cm}^{-3}$ ) was grown before Au contacts were deposited. PL measurements were performed at a lowest sample temperature of 10 K in a He-flow cryostat and as excitation source, the 514-nm line of an Ar ion laser was used. The PL signals were analyzed with a double-grating monochromator, together with a liquid-nitrogen-cooled Ge detector, using a standard lock-in technique. In order to achieve a varying electric field across the dot structures, the diodes were reverse biased. The electric field was calculated from the reverse bias applied and the total thickness of the intrinsic layer, taking the widening of the depletion width into account, assuming that the field was homogeneous over the intrinsic region and disregarding losses originating from the contact and wiring resistance.

Since the Stranski-Krastanov growth mode in the present case is strain induced and the Ge dot formation is a result of

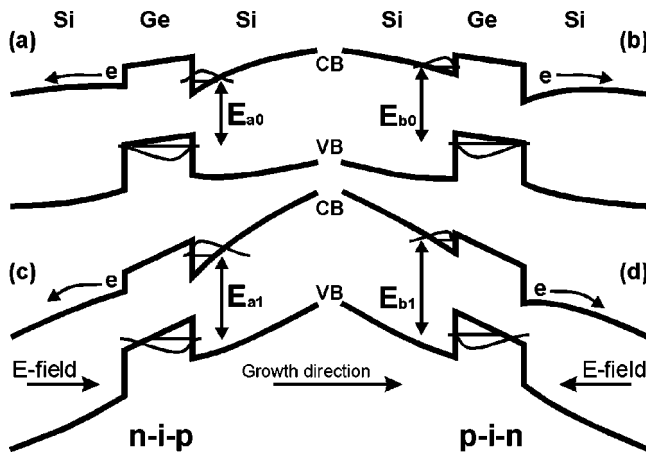


FIG. 1. Schematic illustration of the energy-band alignment in the growth direction through Ge QDs embedded in Si at zero external fields for an *n-i-p* (a) and *p-i-n* (b) diode. Due to the asymmetric strain profile through the structures, there are deeper potentials for the electrons above than underneath the dots. The built-in electric field from the doped layers on each side ensures tilted bands. At applied reverse bias of *n-i-p* (c) and *p-i-n* (d) diodes with Ge QDs, electrons on the *n*-doped side escape while electrons on the *p*-doped side are able to recombine with holes in the Ge dots. The QCSE gives rise to a blueshift of the transition energy under influence of a field, i.e.,  $E_{a0} < E_{a1}$  and  $E_{b0} < E_{b1}$ .

elastic relaxation, the Si above and below the dots exhibits tensile strain.<sup>1,2</sup> It is known that in tensile strained Si, the sixfold degeneracy of the CB is split up into  $\Delta(2)$  and  $\Delta(4)$  bands. The  $\Delta(2)$  valleys are downshifted, which results in a type-II band alignment at the interface between a Ge dot and the surrounding Si.<sup>1,2,8-10</sup> In the valence band (VB), there is a large offset and the holes are confined inside the Ge dot while the electrons are located in the notch potential of the surrounding Si. Consequently, the optical transitions will be essentially spatially indirect in Si/Ge QD structures.

The structural properties were evaluated by AFM measurements on similar but uncapped structures and the Ge dots were determined to be of elongated or square pyramidal shape. The base is surrounded by a Ge rich wetting layer, while the upper part of the dot is allowed to elastically relax to form these pyramidal shapes, giving rise to an asymmetric strain distribution in the surrounding Si during capping. The tensile strain in the Si above the Ge dot should then be higher than in the Si underneath the dot, as has been predicted in several theoretical works.<sup>5-7</sup> Since the magnitude of the tensile strain in the Si determines the size of the downshift of the Si  $\Delta(2)$  valleys, we expect these structures to exhibit an asymmetric energy-band lineup where the deepest electron potential is located right above the center of the Ge dot (see Fig. 1). Interdiffusion of Si and Ge during the growth is always present and will provide gradual changes in the VB and CB, which result in a band lineup with smoothed potential barriers.<sup>1</sup>

When there is a sufficiently strong, built-in and/or external, electric field, the unpaired electrons at the lower energy interface of the Ge dot can escape from the notch potential due to the field and the separation of the electrons and holes

(see Fig. 1). The only possible optical transition is then related to the paired electron and hole at the opposite side of the dot, i.e., on the *p*-doped side of the structure. Consequently, under influence of an electric field, the luminescence from the *n-i-p* (*p-i-n*) diodes involves the electrons in the notch potential above (underneath) the dot (see Fig. 1).

With an electric field  $F$  applied, the shift of the transition energy in a quantum structure due to the QCSE can generally be described by the relation

$$E(F) = E(0) - pF - \beta F^2, \quad (1)$$

where  $E(0)$  is the transition energy at zero fields,  $p$  is the dipole moment, and  $\beta$  is the polarizability of the electron-hole system.<sup>11</sup> At zero field in type-I quantum structures, the dipole moment is close to zero and the polarizability term is predominant, resulting in a parabolic dependence for the QCSE with a quadratic redshift of the transition energy as a function of the electric field. In contrast to type-I quantum structures, a built-in dipole moment is always present in type-II structures, since the electron and the hole are spatially separated. The dipole moment  $p$ , dominates the QCSE in those structures and the field dependence is consequently dominated by the linear term.<sup>11</sup> Figure 1 shows the principles of the QCSE in Si/Ge QDs, where  $E_{a0}$  and  $E_{b0}$  denote the optical transition energies at a zero external field while  $E_{a1}$  and  $E_{b1}$  indicate the transition energy with an applied electric field for *n-i-p* and *p-i-n* diodes, respectively. Even without any external field applied there is a built-in field across the structure due to the doped layers. This electric field, approximately 10 kV/cm, will also produce a small quantum-confined Stark shift. The built-in field is adding a constant value to the total shift and is therefore left outside the analysis of the field dependence. The electron-hole dipole moment is negative in our structures as a consequence of the band alignment and the Ge dot-related emission is thus expected to blueshift at increased electric field, i.e.,  $E_{a0} < E_{a1}$  and  $E_{b0} < E_{b1}$  in Fig. 1. The linear QCSE has several times been experimentally demonstrated for various type-II multiple quantum well structures.<sup>12,13</sup> Two effects compete when the electric field is applied along the growth direction of a quantum structure. First, there is the shift due to the QCSE of the bound states of the electrons and holes as discussed above. Second, the electric field also affects the exciton overlap function and accordingly its binding energy. Hence, the transition energy dependence on the electric field is sensitive to the exciton binding energy as well as the confinement potential profile. In type-I Si/SiGe quantum wells, the electron is weakly confined and the reduction of the exciton binding energy is thought to compensate the QCSE related redshift since the expected redshift is absent.<sup>10</sup> In our type-II structures, on the other hand, the exciton binding energy increases with increasing field which enhances the overlap function since the spatial separation of the electron and hole decreases. There is also a nonlinear up shift of the energy levels as a result of increased confinement of the carriers at an applied field. However, we expect this effect to be small in comparison to the energy shift caused by the dipole moment.

Figure 2 shows PL spectra of the two different structures at 10 K. In order to make a more accurate determination of

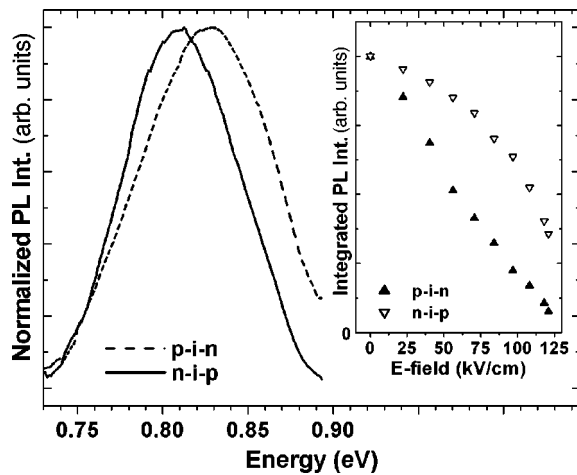


FIG. 2. Normalized PL spectra at 10 K at zero external electric field. The luminescence is centered at 0.83 and 0.81 eV for the *p-i-n* and *n-i-p* structures, respectively. The inset shows the normalized, integrated PL intensity for the two diodes as a function of the applied reverse electric field.

the energy position of the luminescence from Ge dots, broadened due to the inhomogeneous size and composition distribution, the peaks were fitted to Gaussian distributions. Figure 3 shows the resulting energy shift of the Ge dot-related emission as a function of the electric field for the *p-i-n* and *n-i-p* structures. The blueshift of the emission observed with increasing electric field due to the QCSE is approximately linear indicating that the built-in dipole moment is the dominating factor in the QCSE [see Eq. (1)], as expected for this type-II system. We conclude that the reduction of the transition energy due to increased binding energy of the exciton is not large enough to cancel the blueshift of the emission peak but will just decrease the magnitude of the blueshift.

A large dipole moment and hence a large spatial separation of the electron and hole is required to ensure a large QCSE in type-II systems [see Eq. (1)]. Yakimov *et al.* have recently published results of room-temperature photocurrent

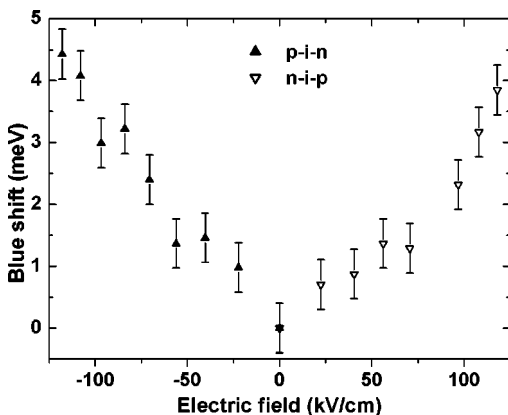


FIG. 3. Observed blueshift of the Ge dot-related luminescence for both *p-i-n* and *n-i-p* diodes as a function of the electric field applied. The field is defined as positive if the direction is from the substrate to the surface contact. The error bars show the accuracy of the fitting procedure.

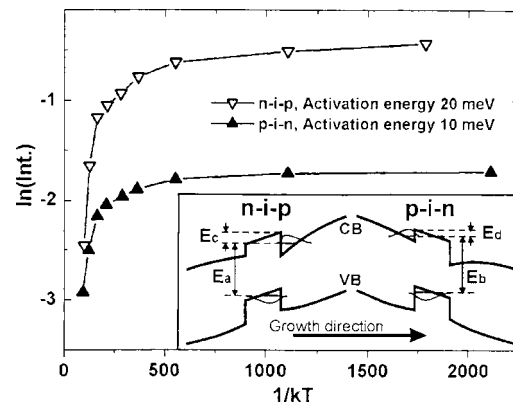


FIG. 4. Arrhenius plot of the temperature dependence of the luminescence intensity for the *n-i-p* and *p-i-n* diodes at zero external electric field applied. The extracted activation energies are different for the *n-i-p* and *p-i-n* structures (as given in the figure). The inset shows a schematic picture of the band alignment for the two diodes.  $E_a$  and  $E_b$  indicate the transition energies while  $E_c$  and  $E_d$  denote the energy barriers for the electrons to escape from the notch potentials.

measurements that have been interpreted in terms of a dramatic Stark shift of the absorption edge for Ge QDs in Si due to an electron-hole separation of 5 nm.<sup>14</sup> However, their structures are quite different from ours: The structures were not grown using the Stranski-Krastanov growth mode, but the Ge islands were instead formed on SiO<sub>x</sub> resulting in islands with a higher height-to-width ratio. The transition energies were very close to the band gap of Si and not around 0.8 eV as in our case. The magnitude of the QCSE in the present study indicates that the electron-hole separation is approximately 0.4 nm.

To further investigate the band alignment, temperature and electric-field-dependent measurements were performed. As discussed above, the geometry and strain considerations imply that the notch potential for the electrons is expected to be deeper above than underneath the Ge dot. Already a glance at the PL spectra in Fig. 2 implies an asymmetry of the band alignment since the dot-related emission for the *p-i-n* structure is blueshifted (0.83 eV) versus the *n-i-p* structure (0.81 eV). Accordingly, our PL results indicate a difference of approximately 20 meV for the CB offset in the upper relative to the lower part of the dot. As shown in the inset in Fig. 4, the deeper electron notch potential above the Ge dot redshifts the transition energy ( $E_a$ ) compared to the transition energy ( $E_b$ ) for the emission originating from the electron potential under the base of the dot.

The asymmetry proposed is further supported by the integrated PL intensity as a function of the electric field across the structures, as shown in the inset in Fig. 2. The quenching of the PL is a result of an increased probability for the electrons to tunnel through the barrier provided by the Ge dot when the electric field is increased. Our measurements show that the quenching of the luminescence is faster for the *p-i-n* diode than for the *n-i-p* when the electric field is increased. The nonlinear behavior of the data in the inset in Fig. 2 is attributed to the exponential dependence of tunneling of electrons on the potential barrier. Furthermore, we

have measured the temperature dependence of the PL intensity for the  $p$ - $i$ - $n$  and  $n$ - $i$ - $p$  diodes. From the Arrhenius plot in Fig. 4 we deduce two different activation energies for the two diodes, approximately 20 meV for the  $n$ - $i$ - $p$  diode and about 10 meV for the  $p$ - $i$ - $n$ . Although the accuracy of these estimates does not allow any quantitative conclusion, the divergence confirms the evidence for different depths of the confinement potentials for the electrons above the center of the dot and underneath the base of the dot, as indicated in the inset in Fig. 4.

In conclusion, we present a study of the QCSE for the type-II Si/Ge QD system based on Stranski-Krastanov growth. A blueshift of the QD emission is observed when an electric field is applied. This blueshift originates from a dominating up shift of the carrier levels due to the QCSE although the transition energy is partly reduced due to an increased exciton binding energy. Both  $p$ - $i$ - $n$  and  $n$ - $i$ - $p$  diodes were studied in order to analyze the QCSE in both field directions. The size of the QCSE indicates a relatively small

spatial separation about 0.4 nm between the electrons and holes and consequently a small dipole moment. The different luminescence properties of the two different diodes in terms of energy position, temperature, and electric-field dependence, are all consistent with the proposed asymmetric band alignment in these structures. From the luminescence peak energy position we estimate that the notch potential is approximately 20-meV deeper for the electrons above the Ge dot relative to the notch underneath, which is in reasonable agreement with the thermal activation energies evaluated for the two transitions. This difference is due to the asymmetric strain profile through the QD structure as a consequence of the QD layer geometry with a wetting layer at the base of the QDs.

This work has been supported by the Swedish Foundation for Strategic Research (SSF) within the NANOPTO Project and INTAS within the NANO-0444-2001 Project.

---

<sup>1</sup>K. Brunner, Rep. Prog. Phys. **65**, 27 (2002).

<sup>2</sup>O. G. Schmidt, K. Eberl, and Y. Rau, Phys. Rev. B **62**, 16 715 (2000).

<sup>3</sup>D. A. B. Miller, D. S. Chemla, T. C. Damen, A. C. Gossard, W. Wiegmann, T. H. Wood, and C. A. Burrus, Phys. Rev. Lett. **53**, 2173 (1984).

<sup>4</sup>G. Bastard, E. E. Mendez, L. L. Chang, and L. Esaki, Phys. Rev. B **28**, 3241 (1983).

<sup>5</sup>J. H. Seok and J. Y. Kim, Appl. Phys. Lett. **78**, 3124 (2001).

<sup>6</sup>M. Grundmann, O. Stier, and D. Bimberg, Phys. Rev. B **52**, 11 969 (1995).

<sup>7</sup>V-G. Stoleru, D. Pal, and E. Towe, Physica E (Amsterdam) **15**, 131 (2002).

<sup>8</sup>Chris G. Van de Walle and Richard M. Martin, Phys. Rev. B **34**,

5621 (1986).

<sup>9</sup>C. Penn, F. Schäffler, G. Bauer, and S. Glutsch, Phys. Rev. B **59**, 13 314 (1999).

<sup>10</sup>Y. Miyake, J. Y. Kim, Y. Shiraki, and S. Fukatsu, Appl. Phys. Lett. **68**, 2097 (1996).

<sup>11</sup>K. L. Janssens, B. Partoens, and F. M. Peeters, Phys. Rev. B **65**, 233301 (2002).

<sup>12</sup>J. S. Park, R. P. G. Karunasiri, and K. L. Wang, J. Vac. Sci. Technol. B **8**, 217 (1990).

<sup>13</sup>H. Haas, N. Magnea, and Le Si Dang, Phys. Rev. B **55**, 1563 (1997).

<sup>14</sup>A. I. Yakimov, A. V. Dvurechenskii, A. I. Nikiforov, V. V. Ulyanov, A. G. Milekhin, A. O. Govorov, S. Schulze, and D. R. T. Zahn, Phys. Rev. B **67**, 125318 (2003).